Mon. Not. R. astr. Soc. (1968) **141**, 219–249.

EXPANDING ATMOSPHERES IN OB SUPERGIANTS—I

*J. B. Hutchings**

(Communicated by the Director of the Cambridge Observatories)

(Received 1968 February 27)

Summary

Radial velocity measurements have been made on high dispersion plates of the Of stars HD 152408 and 151804, and the B1 supergiant HD 152236. In all cases, velocities differ between different ions and between strong lines of H and He I, indicating the existence of extended accelerating atmospheres. In the O stars, P Cygni profiles indicate that the velocities reach 600 km s^{-1} and beyond. Tentative temperature and velocity fields are proposed. In a second paper, theoretical line profile calculations will be presented which confirm these velocity fields.

Introduction. It is generally accepted that the envelopes of high luminosity early type stars are considerably more extensive than indicated by 'standard' model atmospheres. Even in main sequence stars where gravities are high, thin atmosphere models are unable to account for the strengths of the strongest absorption lines. In the very bright supergiants, where gravities are low, they fail completely to produce a realistic picture. The reason for this is that in such stars, the three basic physical assumptions of the models are furthest from being realized. These are, (1) all level populations correspond to states of local thermodynamic equilibrium (LTE), (2) the atmospheric structure is determined by equations of hydrostatic equilibrium, and (3) the radiative flux is constant at all heights, and given by the Milne–Eddington transfer equation.

The solution of the problem without these assumptions is difficult and it is desirable to try to form an empirical picture of the atmospheres of OB supergiants in order to decide what physical processes and assumptions do apply in such cases. It was with this in mind that a study was undertaken of high dispersion spectrograms of the very bright OB stars in the southern galactic cluster NGC 6231. The best and most numerous spectrograms were of the Of stars HD 151804, 152408 and the B1 supergiant HD 152236, all of which have absolute magnitude -7 or brighter.

A detailed investigation of the line velocities and profiles produced evidence that all three stars have extensive and expanding envelopes. The mean radial velocities of absorption were found to differ between different ions and elements, and between strong lines of H and He I. The strongest lines have P Cygni type emission components and the conditions of radiation dilution and density under which they are formed can be deduced from their profiles. In this way the relations between excitation temperature, velocity and height are established.

We begin therefore with a brief discussion of the formation of spectral lines under extended atmosphere conditions and the interpretation of observations.

* Present address: Dominion Astrophysical Observatory, Victoria, British Columbia.

The observational evidence is then presented for the three stars in turn, and the states of their atmospheres deduced.

The formation of strong lines in an extended atmosphere. Many of the observed lines have P Cygni profiles, which are themselves an indication of an extensive expanding atmosphere. The absorption in such a profile occurs over the stellar disc, or between the observer and the stellar photosphere. Here the radial velocity is greatest and the absorption is therefore blue-shifted with respect to the line centre. The presence of a redward emission component indicates that the atmosphere is moving and extensive, the volume of atmosphere being large enough in relation to the photosphere for scattered light from it to be appreciable. The emission component of the line is formed higher in the atmosphere and over a greater range of radial velocities (with respect to the observer) than the absorption. In the extreme case of an expanding atmosphere much larger than the star the emission component will show all velocities from $+V$ to $-V$, where V is the expansion velocity of the atmosphere, while the absorption component will show (almost entirely) $-V$. Increase in the continuum opacity (electron scattering) of the atmosphere will attenuate the red wing (receding side) of the emission and increase the absorption component redward of $-V$. The occultation by the central disc in a non-infinite atmosphere also diminishes the redward contribution. To obtain an expansion velocity from a P Cygni profile all these effects must be allowed for and the only way of doing this is to compute some sample profiles. This computation will be described in detail in a second paper and at present we say only that there is no simple way of interpreting the observed velocities without knowing the stellar atmospheric velocity field in some detail. At best, the process of interpretation of such profiles must be one of successive approximation.

In addition to pure scattering, there is the possibility of enhanced emission arising from non-equilibrium populations of energy levels. It is these effects that Wellmann (1951) has calculated for high dilution cases for He I.

In general, levels whose strongest transitions are observed in emission are likely to have non-equilibrium populations and thus represent conditions in the outer parts of the atmosphere. Wellmann's results for He I are summed up by:

(1) The relative populations of ground and $2\ ^1S$ states are independent of dilution, while other singlet levels are depopulated.

(2) The metastable level $2\ ^3S$ gains by a factor 10 to 20 relative to the ground state and is independent of dilution at high dilution.

(3) Other triplet states are depopulated, except for $n\ ^3P$, which gain by a factor 10 to 20.

This means that in a dilute radiation field the levels $2\ ^3S$, $2\ ^3P$ and $3\ ^3P$ are by far the most heavily populated. Since the lines with $3\ ^3P$ as lower level are all in the infrared they may be disregarded in the present considerations. In the limiting case where gas and radiation temperatures are equal the $2\ ^3P$ population rises with temperature while for the $2\ ^3S$ population the reverse is true. Where the gas temperature is lower than the radiation temperature there is an inverse correlation of level populations with radiation temperature. As the outer atmospheric layers are expected to have the lowest temperatures the strong $2\ ^3S$ lines should represent these parts of the star. These lines (with relative strengths in brackets) are 3888 Å (20) and 3187 Å (8).

The $2\ ^3P$ lines are more highly populated and cover a greater range of tem-

peratures. These may therefore show a greater range of the outer atmosphere, probing to greater depths as the opacity in the line decreases. These lines, with strengths by C. E. Moore, are,

5875	4471	4026	3819	4120	4713	3705	3867 Å
(11)	(7)	(5)	(5)	(4)	(4)	(4)	(3)

Other strong transitions may have a significant contribution from the upper atmosphere, in spite of dilution effects. The strongest lines not mentioned so far are 6678 Å (6) and 4921 Å (4). These both have the lower stage 2 ^1P. The line at 5015 Å has similar strength to 6678 Å but comes from the 2 ^1S level which is consistently 2 to 3 times less populated than 2 ^1P.

Finally, the tendency of these lines to form emission components under different conditions of dilution are given quantitatively in Wellmann's results and are summarized as follows. (The dilution W is defined as light flux/flux at photosphere and is thus geometrically related to distance from the stellar surface.)

2 ^1P lines: strong emission for $W <$ about 0·3.

2 ^3P lines: strong emission for $W < 0{\cdot}1$.

2 ^3S lines: emission only at very low W and high radiation temperature.

Thus the strength of the emission associated with the strong He I lines gives us a measure of the height above the star at which it was formed and defines a velocity–height relationship.

Similar work was done on Balmer line formation by Menzel *et al.* (1937, 1938). Applying Wellmann's methods to their results shows that Balmer lines have a strong emission tendency for $W < 0{\cdot}1$, with no great difference between individual lines. Lines with no sign of emission must be formed at values of $W = 0{\cdot}5$ or greater.

The observations in general. The spectrograms were all taken at the coudé spectrograph of the Radcliffe 74-in. reflector. Fourteen plates are in the blue region of the spectrum (between 3100 and 4900 Å) on IIaO or ISBS emulsions, in the grating second order spectrum (6·83 Å/mm). Five each of these are of HD 152236 and 152408; four are of HD 151804. There are also three 103aF plates covering the region 4500 to 6750 Å, of HD 152236, in the first order spectrum (13·7 Å/mm). Seven of the blue plates were taken for the purpose of this work and the remainder for radial velocity work some years earlier. The older plates are generally more exposed and less grainy.

Radial velocity measurements were made on all medium and strong lines and true intensity profiles derived for all strong lines. The photometry was done by computer, using a program designed for the digital output from the Cambridge microphotometer. This paper uses only a small part of these measurements and description of the computer program is postponed to a later occasion. The computerized reduction procedure is as accurate as any manual method, introducing a maximum operational error of 1 per cent of the continuum intensity, provided that a large proportion of each spectrum is substantially free of lines.

The radial velocity measurements are presented for the three stars in full and used to deduce the expanding state of the three stellar envelopes.

HD 152236. The star is the brightest member of the cluster NGC 6231. $m_v = 4{\cdot}88$, spectrum B1 Ia–O, $M_v = -8$ (Hutchings 1966). The spectral lines are very sharp and radial velocity measurements relatively accurate. Five blue plates

TABLE I

HD 152236. *Measured velocities of spectral lines*

Identification	λ	Velocities of lines or measured λ					Remarks
		6/7/60	9/8/60	10/8/60	28/6/66	27/7/66	
Co I	3086·77	—	(−43)	—	—	—	Measurement inaccurate
Mg I	3093·05	—	(+34)	—	—	—	Measurement inaccurate
Mg I	3096·92	—	(+5)	—	—	—	Measurement inaccurate
He I	3187·75	−70	(0)	—	—	—	Measurement inaccurate
He I	3634·3	—	−36	—	—	−30	—
H 23	3673·76	—	—	−25	—	—	—
H 22	3676·36	−37	—	−25	—	—	—
H 21	3679·36	−29	−16	−17	—	—	—
H 20	3682·81	−29	−16	−25	−33	—	—
H 19	3686·83	(−29)	(−8)	−33	−58	—	Close to Fe I calibration line
H 18	3691·56	−37	−24	−33	−42	−21	—
H 17	3697·15	−29	−24	−25	—	−21	—
H 16	3703·86	(−29)	(−8)	—	—	(−13)	Bad blend with He I, O III (?)
He I	3705·1	(−45)	(−32)	—	—	(−29)	Blend with H 16
H 15	3711·97	3712·2	−16	−25	(−17)	−21	Blend with O II 3712·75
H 14	3721·94	−37	−24	−41	−33	−29	—
	—	—	3718·0	—	3717·5	—	Identity?
O II	3727·33	−21	−28	−33	−41	—	—
H 13	3734·37	−37	−32	−37	−41	−29	—
H 12	3750·15	−45	−40	−49	−49	−29	—
H 11	3770·63	−45	−40	−41	−41	−21	—
H 10	3797·90	−45	−40	−41	−41	−29	—
	—	3806·0	3806·3	3806·2	—	—	Faint, partly due to He I 3805·77?
He I	3819·60	−37†	−24	−33	−40	−21	† Shortward wing present
H 9	3835·39	−51	—	−41	−48	−37	—
He I	3838·09	−21	(−8)	(−9)	−17	—	Blend with N II 3838·39?
He I	3867·55	—	−36	−25	−32	—	—
He I	3871·82	3873·2	−16	−33	−40	—	—
O II	3882·20	−5	—	−13	−9	−37	—
He I	3888·65	—	—	(−390)	(−290)	—	—
	—	(−160)	(−230)	(−250)	(−250)	(−230)	—
	—	(−44)	(−77)	(−75)	(−32)	(−55)	Blend with H 8
H 8	3889·05	−28, −74	(−24)	(−13)	(−10)	(−21)	Blend with He I
He I	3926·53	−24	—	−25	—	—	—
Ca II	3933·67	−13	−16	−13	−9	−21	Interstellar
N II	3955·85	−27	−20	−25	−32	—	Blended?

1968MNRAS.141..219H

TABLE 1. (*continued*)

Identification	λ	Velocities of lines or measured λ					Remarks
		6/7/60	9/8/60	10/8/60	28/6/66	27/7/66	
He I	3964·73	−36	−32	−40	−32	−21	—
Ca II	3968·48	−13	−16	−10	−24	−21	Interstellar
Hε	3970·13	(−66)	(−70)	(−67)	(−47)	(−51)	Blend with Ca II
O II	3973·26	−21	−24	−32	−32	−13	—
N II	3995·00	−35	−24	—	−32	−29	—
He I	4009·27	−28	−24	−32	−31	−28	—
He I	4026·3	(−270)	—	(−370)	(−270)	—	Shortward limit
	—	−57	−39	−47	−46	−43	—
N II	4035·09	−20	—	—	—	—	—
N II	4041·52	−20	—	—	—	—	—
N II	4043·54	−20	—	—	—	—	—
	—	—	4057·0	—	—	—	Identity?
	—	—	4050·9	—	—	—	Identity?
O II	4069·07	−6	−24	−18	−31	−28	—
O II	4072·16	−13	−17	−18	(−9)	—	—
O II	4075·87	−13	−17	−25	−24	−21	—
Si IV	4088·86	−13	−17	−18	−31	−21	—
N III	4097·31	−6	−24	−25	(−38)	—	—
Hδ	4101·75	(−160)	—	—	—	—	Shortward wing
	—	−68	−82	−80	−68	−57	Blend with N III 4103?
Si IV	4116·10	−6	−17	−11	(−38)	—	—
	—	4119·3	—	—	—	—	O II, N II blend?
He I	4120·9	−34	(−46)	−32	(−45)	(−72)	Weak O II blends
He I	4143·76	−34	−31	−32	−37	−28	—
N II	4227·75	−13	—	—	—	—	—
N II	4237·0	—	—	−32	—	—	—
N II	4241·79	−20	−17	—	—	−14	—
O II	4253·9	(−41)	(−38)	(−46)	(−44)	(−35)	Blend with Si III
	—	—	4262·3	—	—	—	Identity?
C II	4267·13	—	−24	−32	—	—	—
	—	4284·9	4285·1	4285·0	4284·9	4285·1	Si III, O II, Fe III blend
O II	4317·14	−20	−17	−25	(−16)	−14	—
O II	4319·63	−20	−17	−18	−23	—	—
Fe II	4332·88	—	(−31)	(−26)	—	—	Identity dubious
O II	4336·87	—	−10	−18	−30	—	—
Hγ	4340·47	(−350)	—	—	—	—	Shortward wing
	—	(−160)	—	—	—	—	Plus blends
	—	−82	−99	−100	−91	−89	—

TABLE I (*continued*)

Identification		λ	Velocities of lines or measured λ 6/7/60	9/8/60	10/8/60	28/6/66	27/7/66	Remarks
O II		4345·56	−27	−24	−32	−36	−21	—
O II		4347·4	(−13)	—	—	—	—	Faint, blended?
O II		4349·43	−27	−17	−25	−29	−21	—
O II		4351·4	−27	—	−25	−29	—	—
		—	4354·4	—	—	—	—	Identity?
		—	4361·5	—	—	—	—	Identity?
O II		4366·90	−20	−17	−18	−23	−21	—
		—	4372·1	—	4372·2	—	—	Identity?
He I		4387·93	−33	(−44)†	−39	−36	−28	† End of plate
O II		4414·91	−26	—	−18	−29	−8	—
O II		4416·98	−26	—	−25	−16	−8	—
Band		4430	4428·2	—	4429·0	4427·4	—	Interstellar
N II		4447·03	−26	—	−18	−22	−14	Diffuse at times
He I		4471·6	−470	—	−460	—	—	Shortward wing
		—	−330	—	—	−320	—	Shortward wing
		—	−73	—	−72	−61	−61	—
Mg II		4481·23	−46	—	−38	(−16, −62)	(−21)	—
Si III		4552·65	−29	—	−25	−31	−27	—
Si III		4567·87	−33	—	−25	−35	−21	—
Si III		4574·78	−26	—	−25	−35	−21	—
O II		4590·97	—	—	−25	−31	−15	—
O II		4596·17	—	—	—	−35	−21	—
N II		4601·48	—	—	−25	−35	−27	—
N II		4607·15	—	—	−31	−29	−24	—
N II		4613·87	—	—	−19	−29	−27	—
N II		4621·39	—	—	−25	−29	−27	—
N II		4630·54	—	—	−31	−35	−27	—
O II		4638·85	—	—	(0)	−35	−37	Blended
		—	—	—	—	4641·9	4641·9	Identity?
N II		4643·08	—	—	(−25)	—	(−26)	Blend with O II
O II		4649·14	—	—	−31	−28	—	C III blend?
O II		4661·64	—	—	−25	—	−17	—
O II		4676·23	—	—	−19	—	—	—
Hβ		4861·33	—	—	—	(−310)	(−320)	Shortward absorption
		—	—	—	—	—	(−230)	Components
	e	—	—	—	—	−127	−145	—
	e	—	—	—	—	+10	+4	—
He I		4921·93	—	—	—	(−58)	−39	End of plate

TABLE I (*continued*)

HD 152236. *Red plate measurements*

Identification	λ	Line velocities or measured λ 10/8/60	11/8/60	17/4/62	Remarks
Si III	4552·65	−32	−32	—	—
Si III	4567·87	−32	−18	—	—
Si III	4574·78	−25	−19	—	—
N II	4607·15	—	−19	—	—
N II	4613·87	−38	−19	—	—
N II	4621·39	−32	−25	—	—
N II	4630·54	−31	−19	—	—
O II	4649·14	−13	−12	—	C III blend?
O II	4661·64	−19	−6	—	—
O II	4676·23	−13	−6	—	—
Hβ	4861·33	−300	—	—	Shortward absorption
		−118	−118	—	Components
	e	+25	+52	—	—
He I	4921·93	−53	−40	—	—
N II	4994·36	—	−13	—	—
N II	5001·3	—	−19	—	—
N II	5002·69	—	−19	—	—
N II	5005·14	—	−25	—	—
N II	5010·62	(−19)	−31	—	—
He I	5015·68	—	(−91)	—	Identity?
N II	5045·10	−31	−28	—	—
He I	5047·74	−31	−37	—	—
N II	5666·64	−41	−36	−14	—
N II	5676·02	−30	−36	−33	—
N II	5679·56	−41	−46	−17	—
N II	5686·21	−26	−36	−22	—
	—	5696·5	5696·4	5695·8	Identity?
N II	5710·76	−36	−30	−8	—
	—	5722·6	—	5722·4	Identity?
Si III	5739·76	−41	−38	−11	—
		—	5780·6	—	Identity?
He I	5875·63	−129	−123	−78	—
	e —	+11	+11	+35	—
N II	6482·17	−31	−42	−49	—
Hα	6562·82	−277	−272	−230	—
	—	−189	−174	—	Double absorption lines
	e —	+2	+2	−11	—
He I	6678·15	−126	−131	−137	—
	—	(−85)	—	−107	Double absorption
	e —	+6	+13	—	—

were measured from the Balmer limit as far as possible towards the red. Lines shortward of the Balmer limit are less well exposed on the plate and often blended and were not considered worth measuring. The r.m.s. error for a line measured on one plate is about 5 km s^{-1}. The strong lines present are almost entirely from H, He I, O II and N II. A few lines of Si III, Si IV, C II, N III and Mg II were also measured. All velocities given are corrected for the Earth's orbital motion. Where lines are unidentified the measured wavelength is given. Values in brackets have half weight.

The red plate data are less accurate because of the lower dispersion. The lines Hα, Hβ and He I 6678 and 5875 have P Cygni structure. The letter 'e' in the identification denotes an emission component.

There are several interesting features in these results. The first of these is in Fig. 1 which shows radial velocity variation along the Balmer series. The lines Hα to Hε show a rapid decrease in velocity, and the higher lines seem to tend more gradually to an asymptotic limit. The value of this limit is estimated and

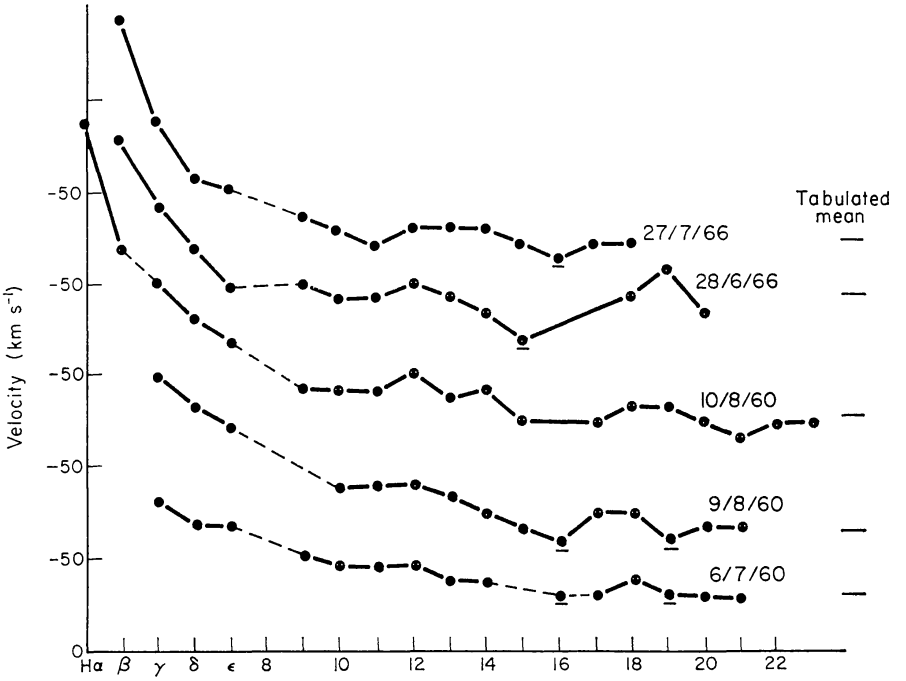

FIG. 1. *Balmer line radial velocities in HD* 152236.

given with standard errors in the following table. The velocities of the stronger Balmer lines are discussed later. The table also shows weighted means of velocities of He I (weaker lines only—4471, 4026, 3888, 5875, 6678 and 4921 excluded—see later), O II and N II, with standard deviations. Fig. 2 illustrates these results. Figures in brackets give the numbers of lines measured in each group.

Date	He I	O II	N II	H	
6/7/60	31·9±2·1 (9)	19·0±1·6 (15)	22·6±2·5 (8)	33±3	
9/8/60	29·4±2·3 (11)	20·2±1·6 (12)	20 ±2 (3)	18±5	
10/8/60	34·1±2·6 (8)	21·2±1·7 (21)	27·0±1·7 (10)	25±3	
10/8/60	—	15 ±2 (3)	32·4±1·9 (11)	—	(red)
11/8/60	—	8 ±2 (3)	27·7±2·3 (16)	—	(red)
17/4/62	—	—	24 ±6 (6)	—	(red)
28/6/66	34·0±2·5 (9)	27·5±1·7 (20)	30·4±1·5 (8)	43±7	
27/7/66	26·4±1·5 (8)	21·4±2·6 (14)	23·2±1·8 (10)	22±3	

We see at once that the radial velocities of the lines of the first three elements are systematically different, while the limiting velocity in the Balmer series varies in a more random fashion. These results are similar to those reported by Merrill (1949) who found a Balmer line velocity progression in the Ape star HD 218393 and Sanford (1947) who found different velocities for Balmer lines, He I, C II, Na I and Na II ions in Rigel (B 8 Ia). The excitation potentials of the lower states of the lines measured are as follows:

H	Balmer lines 10·15
He I	20–21
N II	18–23
O II	22–31

This strongly suggests a systematic increase in radial velocity (towards the observer) with decrease in excitation temperature. That is, an increase in velocity with distance from the surface of the star, assuming the excitation temperature falls monotonically.

A check was made to see whether blends in the lines could be the cause of the apparent correlation, as approximately the same group of lines was measured in all plates of the same spectral region. However, all blends not already accounted for were very weak and were not located so as to give the systematic differences measured. The red plate of 10/8/60 gives a higher N II mean than the blue plate (a few hours later). This too was checked in relation to blends and it was concluded that much of the effect is accounted for by random (grain and measuring) errors. Stronger evidence would be required to indicate a definite change in velocity in a short time.

The strong Balmer lines. We now turn to the Balmer lines Hα to Hε (Figs 2 and 3). The *gf* values for the lines are 2·51, 0·95, 0·36, 0·17 and 0·10 respectively. With the increasing Balmer number the line strengths decrease, or in other words, the opacity of the atmosphere in the line decreases. This means that the profile observed in Hα is formed high in the atmosphere (closest to the observer), Hβ further down, and so on. Differences of velocity between them may therefore give evidence of velocity changes with height within the atmosphere. The Balmer lines from about Hε to the Balmer limit are all formed in a relatively shallow range of depth where the rate of change of velocity with height is small. The errors of measurement then become as large as the differences in velocity and only a mean or asymptote can be found. The same is unfortunately true for the N II and O II lines, which are formed even further down in the atmosphere.

It is again necessary to check whether the effect measured cannot be ascribed to some other cause. In the case of the strong Balmer lines the danger is of the absorption centre being shifted by a redward emission component. Hα certainly has a very strong emission component (some five times the absorption strength). Hβ has a much weaker component (about equal to the absorption strength), but all the other Balmer lines have no emission peak or asymmetry to suggest the presence of emission in any strength. The fact that the velocity series proceeds at least as far as Hε is strong evidence for its reality. In any case the high velocity

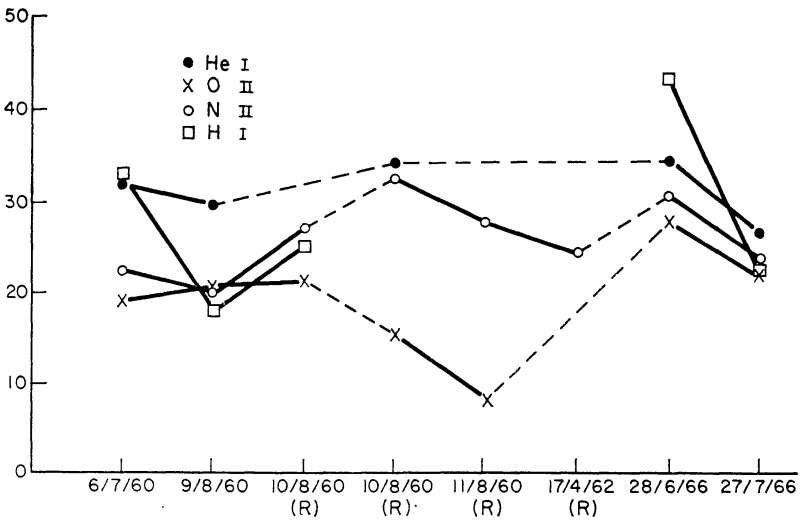

FIG. 2. *Mean velocities of ions in HD* 152236.

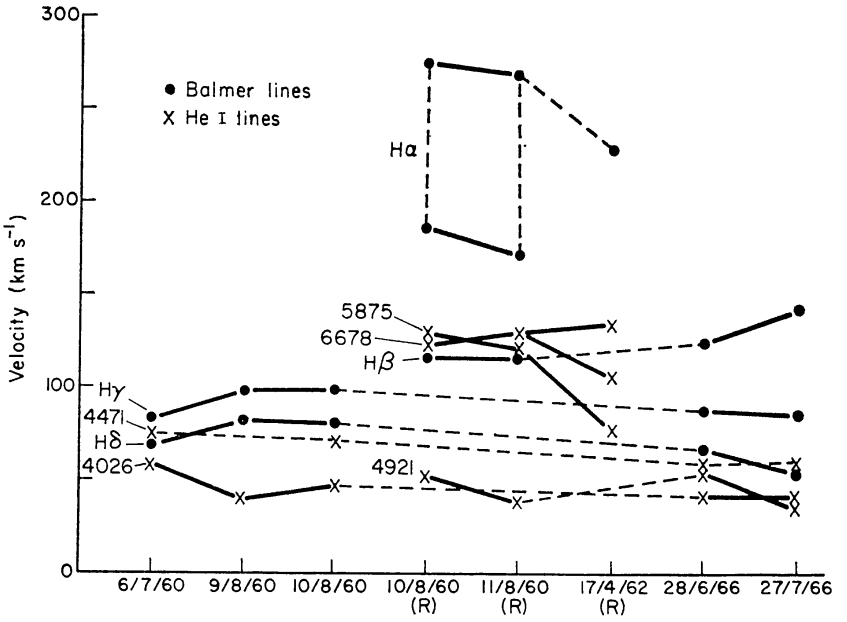

FIG. 3. *HD 152236 high velocity lines.*

shifts are larger than the absorption line width (typical Balmer half-width is 1·8 Å), so that filling in by absorption is not sufficient explanation of the effect. If Hγ or higher lines were simply filled in by an emission component, the pure

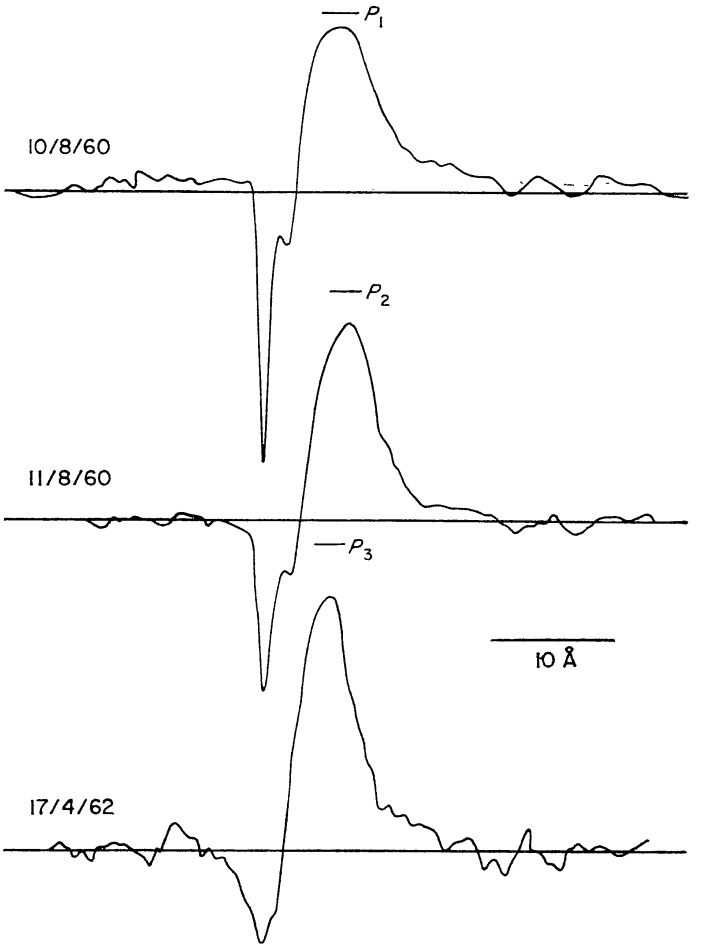

FIG. 4. *Unreduced tracings of Hα in HD 152236. $P_{1, 2, 3}$ represent complete photographic darkening.*

absorption component of these lines would be much wider than any other in the spectrum. We thus seem quite justified in regarding the radial velocities shown by the absorption lines Hα to Hε as real. Finally, the existence of the P Cygni type profiles of Hα and Hβ is itself indication of an expanding atmosphere.

Two of the Hα profiles are bifurcated (Fig. 4) with centres about 100 km s^{-1} apart, while the third appears as a single broader profile with velocity midway between the values of the components of the others. This suggests a layering or fragmentation of the atmosphere at great heights above the star. The emission strength too is seen to be variable, but photographic saturation makes it very difficult to measure the extent of variation, on the present plates.

The strong He I *lines.* The observed strong lines are as follows, with C. E. Moore's strengths in brackets:

2 ^3S lines	3888 (20), 3187 (8)
2 ^3P lines	5875 (11), 4471 (7), 4026 (5)
2 ^1P lines	6678 (6), 4921 (4).

Most of these warrant individual attention.

3888 Å. This line, blended with H8 at 3889·05, shows a very peculiar behaviour, illustrated by the tracings in Fig. 5. The relative stability of the remainder of the Balmer series suggests that the changes result from the He I line, a conclusion supported by measurements in other stars, discussed below. However, the extent of the blending is such that it is difficult to separate the components, especially as it appears that the He I line sometimes splits into more than one component. The shifts indicate variable velocities, of the order of 100–200 km s^{-1}, with no indication of any emission component.

5875 Å. In all three red plates the line has a strong P Cygni profile, with velocities of absorption −129, −123, and −78 km s^{-1}. These velocities correspond closely

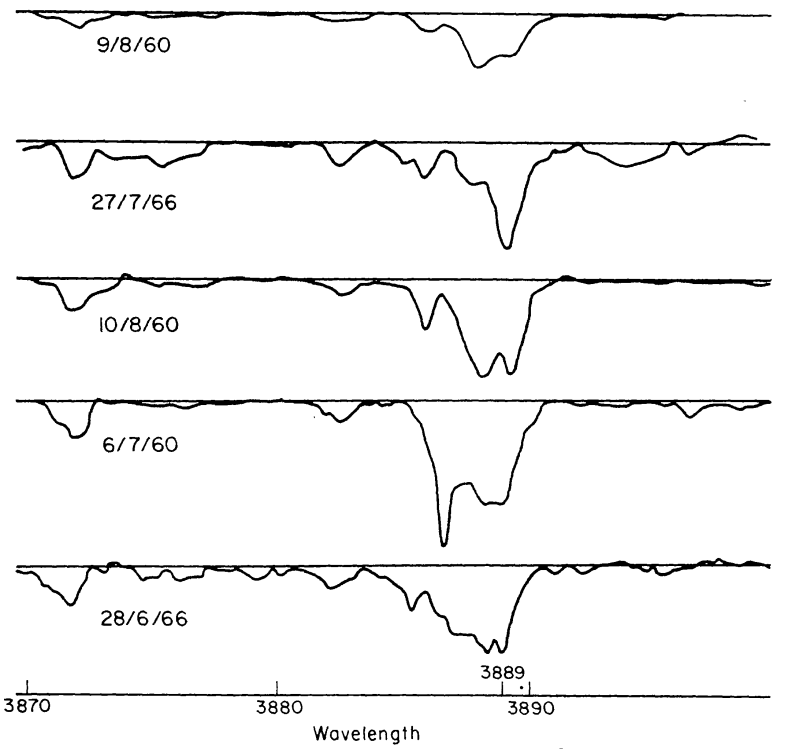

FIG. 5. *Unreduced tracings of blend at* 3888 *Å in HD* 152236.

to the Hβ velocities of absorption measured on the same plates (first two, velocities −118 km s^{-1} for each). Although the grain level of the red plates is high, there appears to be a short wavelength absorption wing to this line on all three plates.

4471 Å. This, the strongest He I line in the blue region, is formed by three features—4471·48 (6), 4471·69 (1) and 4469·92 (forbidden). The 4469 component is generally considered to be present in sufficient strength to account for the asymmetry observed in many sharp-lined B stars. This asymmetry is stronger and more extensive in HD 152236 but it is not possible to determine whether this results from absorption by high velocity atoms or from blends by 4469 and O II at 4466, 4467 and 4469.

4026 Å. A similar argument holds for the 4026 line which has a definite and apparently variable asymmetry in the expected direction, but this is possibly a result of a blend with the He I line at 4023 Å. In the light of similar evidence in the O stars (see below) I am inclined to attribute part at least of the effect to He I absorption in the upper atmospheric layers. In any case the radial velocities indicated by the main lines at 4471 and 4026 are consistently much higher than those of the other He I lines, as indicated in Fig. 3.

There are two other strong He I lines with high absorption velocities. These are at 6678 and 4921 Å, strongest of the 2 ^1P transitions. The velocities of these lines are plotted in Fig. 3. The 6678 line has the higher velocity and a small variable emission contribution on the long wavelength edge.

The remaining spectral lines. The conclusion seems inescapable that the atmosphere of HD 152236 is accelerating away from the star. The radial velocity of the star itself must therefore be inferred and is presumably close to the −25 km s^{-1} indicated by the O II and N II lines. The high ionization lines Si III, Si IV and N III may indicate the velocity near the surface, which would then be about −21 km s^{-1} (mean values are −19, −22, −20, −21, with −33 on 28/6/66). However, as the spectra of these ions are not complete and these represent the strongest transitions, they may be misleading.

The Mg II line 4481 is presumably formed at about the height of the stronger Balmer lines, as its excitation potential is 8·8 V. The velocities of the line are not very reliable, but are consistently high (−48, −64, −39).

The calcium H and K lines and the sodium D lines are very strong and mainly interstellar in origin. The radial velocities of the lines are zero within measuring error. There is in most cases a weak shortward component of the line, which may be stellar and in some cases the main absorption has two close components of almost equal strength. The weighted mean stellar velocities are Na I −43·0 ± 3·6 and Ca II −45·3 ± 3·0 km s^{-1}.

The atmosphere of HD 152236. We now attempt to construct a picture of the velocity field in the atmosphere of HD 152236. Fig. 6 shows a plot of velocity—excitation temperature for the lines measured. The O II, N II and He I lines have naturally by far the greatest weight and lines in the diagram are marked heavily at the temperature at which most of the measured lines should be formed. The temperature scale is obtained using the Boltzmann and Saha equations, thus making the (almost certainly unjustified) assumption of thermodynamic equilibrium. However, the measurements fit together to form a very strong picture of an accelerating inner atmosphere.

The outer atmosphere is defined by individual lines (Fig. 7), using the dilution–

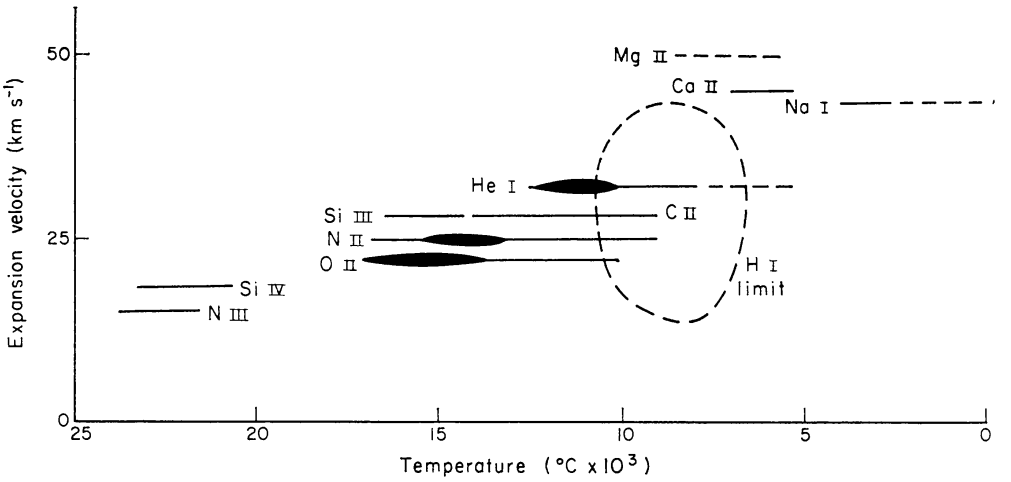

FIG. 6. *Velocity–temperature diagram for ions in HD* 152236. *Thick lines indicate where most of the lines are formed.*

emission strength relations derived by Wellmann. From its strength the 6678 line must be formed at about $W=0\cdot5$, which corresponds to a distance of about 0·3 radii from the photosphere. The 5875 line however appears to have been formed at W about 0·1, which places it at some two radii from the photosphere. The 3888 line probably come from W values 0·1 and greater. The other high velocity lines all most be formed below 0·3 radii and are used to fit the inner and outer atmospheres together, by matching velocities of expansion. From the Balmer lines with emission components, Hβ is placed at $W=0\cdot5$, where the velocity ties in satisfactorily with He I 6678 at about 130 km s^{-1}. Hα is probably formed over the entire depth from $W=0\cdot1$ to 0·25 and higher Balmer lines at progressively smaller heights below 0·3 radii.

The variable bifurcation of Hα and the peculiar variation in He I 3888 indicate that the velocity at greater distances from the surface is extremely variable, apparently splitting into two sharply defined gas streams. The velocity of He I 5875

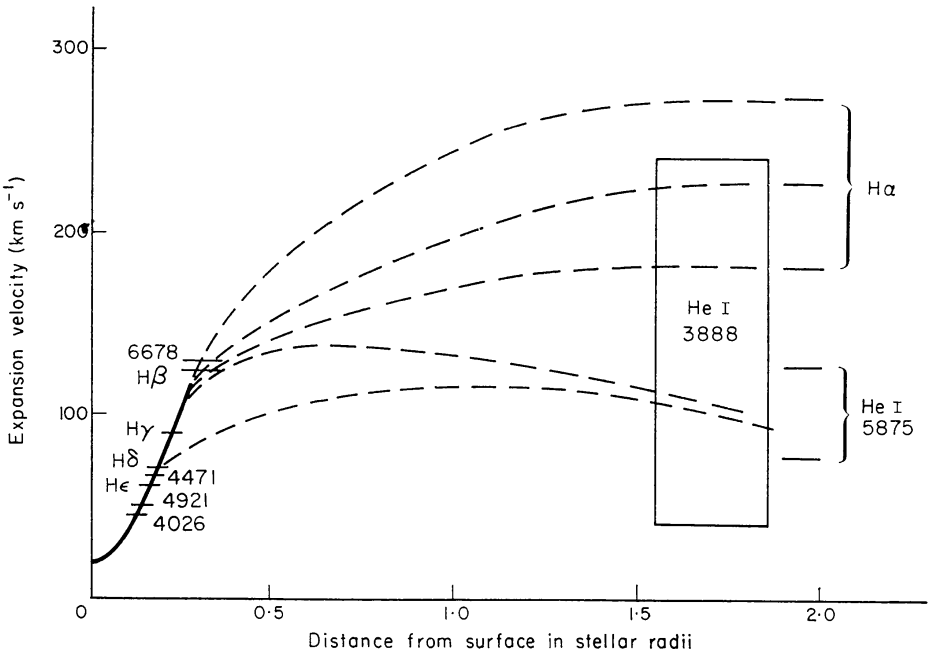

FIG. 7. *HD* 152236 *velocity field from high velocity lines.*

is also seen to be variable, but over a lower range. This may indicate the formation of a third gas stream, which would be unlikely to show up in Hα owing to the strength of its emission component. The Hβ profiles are generally poorly exposed; however, in all cases the absorption appears uneven and asymmetrical and it may be that the gas streams begin to separate at this height. The Hβ blue-shifted absorption corresponds to expansion velocities up to 300 km s^{-1}, but possibly there are blends of O II and N III lines here. (There is however little sign of the strongest members of these O II and N III multiplets, at 4864 and 4867 Å). The Hβ and He I 5875 emission components are bifurcated on the 10/8/60 plate, again suggesting the existence of two gas streams. This interpretation is speculative but has a considerable degree of plausibility, as the gas streams would be unlikely to be constant in any way.

Finally, the velocity field in Fig. 8 is proposed. The excitation temperature is made to approach an asymptote in the region of 7000 °C. However, this is merely an arbitrary starting value for the process of successive approximation in theoretical work to be discussed in a later paper. The different gas streams may well have different excitation temperatures, which could explain the apparently high dilution of the 5875 line.

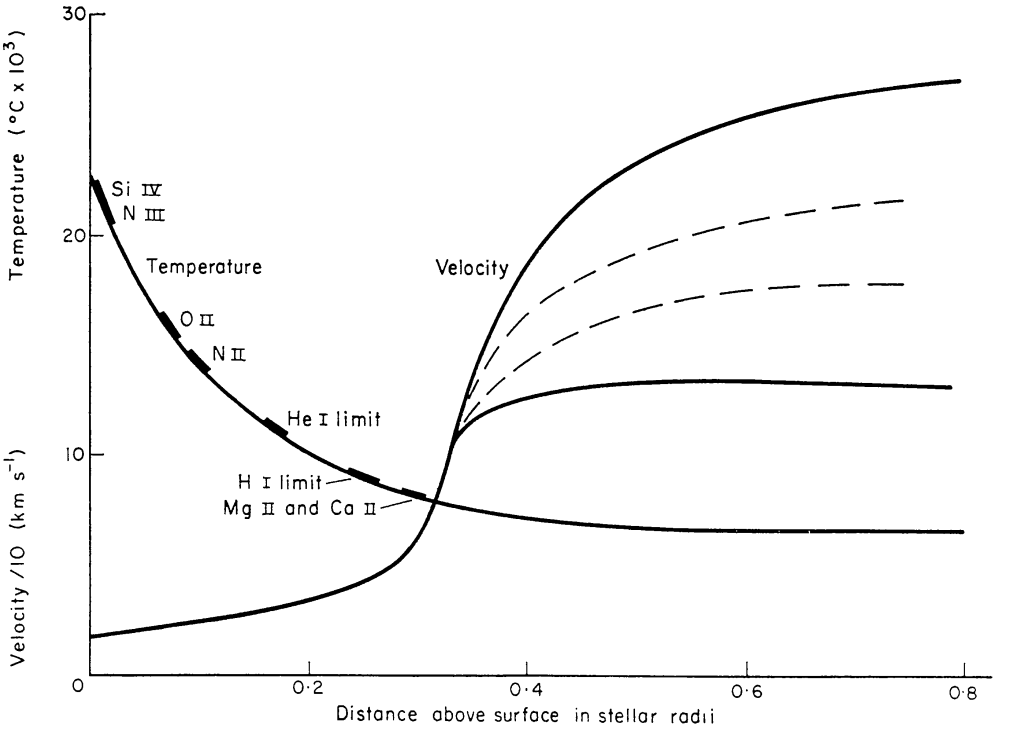

FIG. 8. *Deduced temperature and velocity fields for HD* 152236.

Other published evidence. The radial velocity of the star has been given a single value by various workers, as follows:

Wilson (1953)	star −26	interstellar lines −11
Evans *et al.* (1959)	−34 ± 1·2 (4 plates)	−11
	Hβ emission +1	
Eggen (1958)	−30·0	
Rubin *et al.* (1962)	−26·2	
Buscombe (1962)	−6 to −34 (6 plates)	−9

These are all quite unremarkable considering the fact that probably not all the figures were obtained with the same lines. The consistency of the figures of Evans

et al. is perhaps slightly surprising as they are taken from four different plates. Code & Houck (1958) remark on the strength of the O II lines in this spectrum and the N II 4631 line, rarely seen in Ia supergiants. The entire multiplet of N II lines of which 4631 is a member is present in the measured spectra.

There are only two reports of variability in the star. It is listed in Gaposchkin's variable stars (1938) and Cousins (1952) reports variation in magnitude of $0^m \cdot 05$. Buscombe (private communication) reports finding longward emission on two high dispersion spectra at both Hβ and Hγ, increasing in strength from 3 to 7/8/66. Radial velocity measurements by Buscombe on these plates show the same differential velocity effect as reported here and the Balmer velocity progression. For the two plates, mean velocities of He I, N II, and O II are $-27 \cdot 2$ (7), $-24 \cdot 9$ (9), $-20 \cdot 5$ (20) on 3/8/66 and $-32 \cdot 6$ (7), $-27 \cdot 6$ (14), $-23 \cdot 6$ (18) on 7/8/66. Buscombe & Kennedy (private communication) also report that the effect is recognisable on six lower dispersion spectra of the star. In all, they find consistent negative residuals for the lines 3970, 4026, 4101, 4340, 4387, 4471, 4481, 4452 and consistent positive residuals for the lines 4069, 4072, 4075, 4116, 4120, 4143, 4349 and 4416.

HD 152408. This is an Of star (classed by various authors between O7f and O9f), half a degree from the compact nucleus of the cluster NGC 6231; $m_v = 5 \cdot 8$ and M_v is approximately -7. Five high-dispersion spectrograms have been measured, and tracings made of a further four prismatic spectrograms (29 Å/mm at Hγ). The remarkable spectrum has been commented on by a number of workers (e.g. Swings 1942; Struve 1944; Blaauw 1961), although none has investigated it in much detail. The star is similar to P Cygni in having a number of lines with redward emission components (or strictly blue-shifted absorptions) in addition to the characteristic Of emission lines of N III 4634, 4640–1 and He II 4686. Swings put this star (with HD 151804) under the heading intermediate between WR and absorption O stars.

Struve mentioned a strong diffuse unidentified absorption line at 3880 Å, which appeared to be double at times and found a consistent difference between the velocities of emission lines with and without absorption components.

The present measured spectrograms are of considerably higher quality than those available to other workers and show a number of extraordinary features. The strength of the emission lines (C III, Si IV, N III, He I, H I and the unidentified lines at 4485 and 4503) vary rapidly and irregularly. The line at 3880 varies in a peculiar fashion. The He I 4471 and 4026 lines are strongly asymmetrical. Finally there are weak broad emission bands similar to those found in WR stars and broad absorption dips of similar width (some 100 Å), all of which may appear and disappear irregularly.

The line velocities. The table below gives the line velocity measurements from the high dispersion plates. The lines are broader than those of HD 152236 and individual line velocities have standard errors not less than ± 8 km s^{-1}.

These measured velocities immediately bring out several points:

(1) Velocities of all ions are high, and range over 100 km s^{-1} or more.

(2) Although there is a spread in velocities of individual lines of the same atoms or ions, there are also systematic velocity differences between different ions or atoms.

(3) Nearly all velocities vary from plate to plate.

Table II

HD 152408. *Measured velocities of spectral lines*

Identification		λ	Velocities of lines or measured λ					Remarks
			19/5/62	16/7/62	29/6/66	30/8/66	31/8/66	
Si IV	e	3149·56	—	+10	—	—	—	Strong, emission only
Si IV	e	3165·72	—	+38	—	—	—	Strong, emission only.
He I	e	3187·7	—	(+170)	—	—	—	Weak; diffuse shortward absorption
He II		3203·10	−93	−148	—	—	—	Strong
	e	—	+102	+65	—	—	—	—
	e	—	—	3330·2	—	—	—	Identity?
O III		3335·4	—	(−98)	—	—	—	Identity?
O III		3341·4	—	−98	—	—	—	Wide, irregular. N III blend?
	e	—	—	+69	—	—	—	—
		—	—	3353·5	—	—	—	Blend of He I 3354·6 and N III 3354·3
	e	—	—	3362·6	—	—	—	Identity?
N III		3365·79	—	−46	—	—	—	—
N III		3367·36	—	(−81)	—	—	—	Blend?
N III		3374·06	—	(−108)	—	—	—	Blend?
		—	—	3378·1	—	—	—	Diffuse. Identity?
Ti II		3383·76	−18	−8	—	−19	—	Sharp, interstellar
		—	—	3386·0	—	—	—	Diffuse. Identity?
		—	—	3397·1	—	3397·5	—	Strong. Identity?
N IV		3478·69	−17	−63	−43	−54	−36	—
N IV		3482·98	−8	−71	−26	−45	−28	—
N IV		3484·90	(+18)	−55	−1	—	−28	Faint, sometimes blended
		—	—	3486·4	3488·6	—	3488·7	Identity?
He I		3587·3	−85	—	—	(−117)	—	—
He I		3634·3	−57	−88	—	−93	—	Very asymmetrical
		—	—	3693·3	—	—	—	Diffuse, Balmer line?
		—	—	3697·9	—	—	—	Diffuse, Balmer line?
		—	3703·6	3703·9	3704·0	3704·1	3704·1	Very strong blend of O III, H 16, He I
H 15		3711·97	−40	−84	—	−69	(+20)	—
H 14		3721·94	−48	−100	—	−69	(−90)	—

TABLE II (*continued*)

Identification		λ	Velocities of lines or measured λ					Remarks
			19/5/62	16/7/62	29/6/66	30/8/66	31/8/66	
He I		3732·9	—	—	—	—	−110	—
H 13		3734·37	(−105)	−101	−67	−92	−60	He I blend
H 12		3750·15	−63	−79	−66	—	−68	—
	e	—	3754·5	3754·9	—	—	—	—
O III		3757·2	(−110)	(−178)	—	−82	−75	Blend of O III lines
Si IV	e	3762·41	+42	−17	−1	(+25)	−20	Emission line only
He I		3768·81	—	(−111)	—	—	—	Weak, blended with H 11
H 11		3770·63	−89	−91	−73	−75	−75	—
Si IV	e	3773·13	+40	−27	+8	−12	−4	Emission line only
He II		3781·68	—	−43	—	—	—	Identity?
		—	3782·4	—	—	—	—	Identity?
O III		3791·26	—	−91	—	−67	—	—
H 10		3797·90	−46	−75	−71	−75	−90†	† Shortward absorption at −500?
		—	3813·9	3812·0	3813·4	3812·2	3814·0	He II 3813·5 + shortward He I 3819·6?
He I		3819·6	−85	−106	−88	−75	−98	—
	e	—	—	+60	(+70)	—	+58	Emission weak
H 9		3835·39	−86	−97	(−71)	−67	−59	Blend with He II 3833·8, He I 3835·9?
He II		3858·07	−22	−72	−56	−59	−67	—
		—	—	3866·0	—	3869·6	—	Faint
		—	3879·1	3880·3	3880·9	3880·2	3880·4	Very strong, unidentified
H 8		3889·05	(−200)	(−200)	(−230)	(−175)	(−135)	Blend with He I 3888·6
	e	—	+9	+50	—	3888·1	+140	Possibly He I emission. See text
He II		3923·5	−37	−56	−40	−42	−67	—
Ca II		3933·67	−13	−17	−9	−13	−12	Interstellar
N III	e	3934·41	+24	−9	−1	−5	−13	Emission only
N III	e	3938·52	+47	−33	−10	−14	−13	Emission only
N III	e	3942·78	+62	−9	—	—	—	Emission only
		—	—	—	—	—	3958·5	Identity?
He I		3964·73	—	−123	—	−89	−134	—
	e	—	+9	+5	—	—	—	—
Ca II		3968·48	−13	−10	−9	−6	−5	Interstellar
Hε		3970·13	−90	−116	−91	−81	−82	—
	e	—	—	+105	—	(+210)	—	Diffuse

TABLE II (*continued*)

Identification		λ	Velocities of lines or measured λ 19/5/62	16/7/62	29/6/66	30/8/66	31/8/66	Remarks
		—	—	3989·8	—	3979·6	—	Identities?
N III		3998·69	—	—	−180	—	−171	—
	e	—	—	−25	−32	—	—	Weak emission
N III		4003·64	—	—	—	—	−163	—
	e	—	−54	−17	−10	—	−28	Weak emission
He I		4026·19	−95	−115	−129	−102	−116	Weak blend He II 4025·6
	e	—	—	+65	+103	+69	+81	—
		—	—	4036·0	—	—	—	Identity?
N IV		4057·80	−29	(−68)	−31	—	—	—
Ne II		4062·90	—	−68	—	—	—	—
Ne II		4080·48	—	−107	—	—	—	—
	e	—	—	−32	—	—	—	—
		—	—	4082·7	—	—	—	Identity?
Si IV		4088·86	−159	−156	−147	−130	−124	—
	e	—	+2	+19	+31	+9	+16	—
N III		4097·31	−202	−200	−197	−175	−180	Very broad and strong
	e	—	+30	+28	+21	+31	+16	—
Hδ		4101·75	−81	−90	−117	−79	−86	Blend with N III 4103·3
	e	—	+139	+143	+136	+154	+155	Blend with N III 4103·3
Si IV		4116·11	−159	−170	−126	−167	—	—
	e	—	−5	−10	+12	+1	−5	—
He I		4120·9	—	−75	—	—	—	—
		—	—	—	—	—	4129·5	Sharp, interstellar?
		—	—	—	—	—	4131·8	Identity?
N III		4195·70	—	−126	−93	−118	—	—
	e	—	−30	−24	—	+2	—	—
He II		4199·87	—	—	—	(−73)	—	Blend with N III
N III		4200·02	(−90)	(−103)	(−86)	(−88)	(−155)	Blend with He II
Si IV	e	4212·5	—	−17	—	—	—	—
		—	—	—	4249·8	—	4227·7	O II? and Ca II? respectively
		—	—	—	4252·2	—	4298·3	C III?
N III	e	4328·15	—	−37	—	—	—	—
		—	—	—	—	—	4331·7	Identity?
Hγ		4340·47	−166	−187	−167	−164	−165	—
	e	—	+43	+67	+74	+69	+70	—

TABLE II (*continued*)

Identification		λ	Velocities of lines or measured λ 19/5/62	16/7/62	29/6/66	30/8/66	31/8/66	Remarks
	e	—	4345·4	—	4346·2	4345·6	4346·0	Hγ emission ? O II 4345?
N III		4379·09	—	−126	−138	−136	—	—
	e	—	−5	−10	−9	−8	—	—
He I		4387·93	—	−98	−91	−115	—	—
	e	—	−23	+10	—	+32	—	—
Band		4430	4430	4428	4428	4428·5	4430	Interstellar
		4471·6	—	4464·6	−150	—	−205	Strong shortward wing
He I		—	−145	−144	−96	−115	−115	Weak He I 4469 present?
	e	—	+69	+57	+51+105	+92	+79	—
	e	4485·7	−5	−10	−29	o′	−28	Unidentified. ′ absorption at −156
	e	4503·7	−24	−24	+11	+20	−1	Unidentified. λ by Underhill (1966)
N III		4510·92	−118	−111	−97	−94	−108	—
	e	—	—	(+3)	—	+25	+5	—
N III		4514·89	−118	−118	−109	−101	−102	—
	e	—	—	(+29)	—	+25	+32	—
N III		4518·18	−91	—	−69	−67	−88	—
N III		4523·60	−111	−101	—	−134	−108	—
	e	—	—	—	—	−13	—	—
		—	—	4524·5	—	4525·6	—	Identity?
	e	—	—	—	—	4527·9	—	Same line?
		—	—	—	—	4530·7	—	Identity?
N III		4534·57	−105	−111	−93	−108	−108	—
	e	—	+16	−10	—	+39	+32	—
He II		4541·6	−65	−70	−49	−54	−41	—
		—	—	4568	—	—	4597	Identity?
N III	e	4634·16	—	+2	−10	—	−15	Very strong
N III	e	4640–41	(−50)	+20	−10	—	−30	Very strong
C III	e	4647·40	—	—	−3	—	−8	—
C III	e	4650·16	—	—	+23	—	—	—
Si IV	e	4654·1	—	—	+4	—	—	—
He II	e	4685·75	—	—	+10	—	−66+20	Very strong
He I		4713·15	—	—	−73	—	−91	—
	e	—	—	—	+118	—	—	—
Hβ		4861·33	—	—	—	—	(−275)†	† Also absorption at 4839·6
	e	—	—	—	+88	—	+39	—

Fig. 9 shows mean velocities of pure absorption lines of different elements and ions in the five spectrograms and the numerical values are given below with standard deviations. Absorption lines with emission components are shifted by varying amounts according to the strength of the emission and these lines are omitted. (An exception here is Si IV which is in all cases accompanied by emission and is put in for comparison.) The number in brackets are the numbers of lines on which the figures are based.

Date	He I	He II	H	N III	N IV	Si IV
19/5/62	−76 ± 9 (3)	−41 ± 14 (3)	−62 ± 8 (6)	−109 ± 5 (5)	−15 ± 6 (3)	−160 ± 10 (2)
16/7/62	−85 ± 10 (5)	−60 ± 7 (4)	−90 ± 4 (7)	−114 ± 4 (7)	−63 ± 4 (4)	−163 ± 7 (2)
29/6/66	−84 ± 5 (3)	−48 ± 5 (3)	−70 ± 1 (5)	−91 ± 5 (5)	−25 ± 9 (4)	−136 ± 11 (2)
30/8/66	−86 ± 5 (3)	−53 ± 5 (4)	−74 ± 4 (6)	−101 ± 8 (7)	−50 ± 5 (2)	−148 ± 18 (2)
31/8/66	−114 ± 10 (3)	−58 ± 9 (3)	−73 ± 6 (7)	−125 ± 11 (8)	−31 ± 3 (3)	−124 ± 10 (1)

The difference in velocities here are significant, in spite of a scatter in the individual values comprising each mean which is often much greater than the measuring error. It is concluded that the stellar atmosphere is expanding violently and irregularly and that the distribution and excitation of ions is probably much further from equilibrium values than in HD 152236.

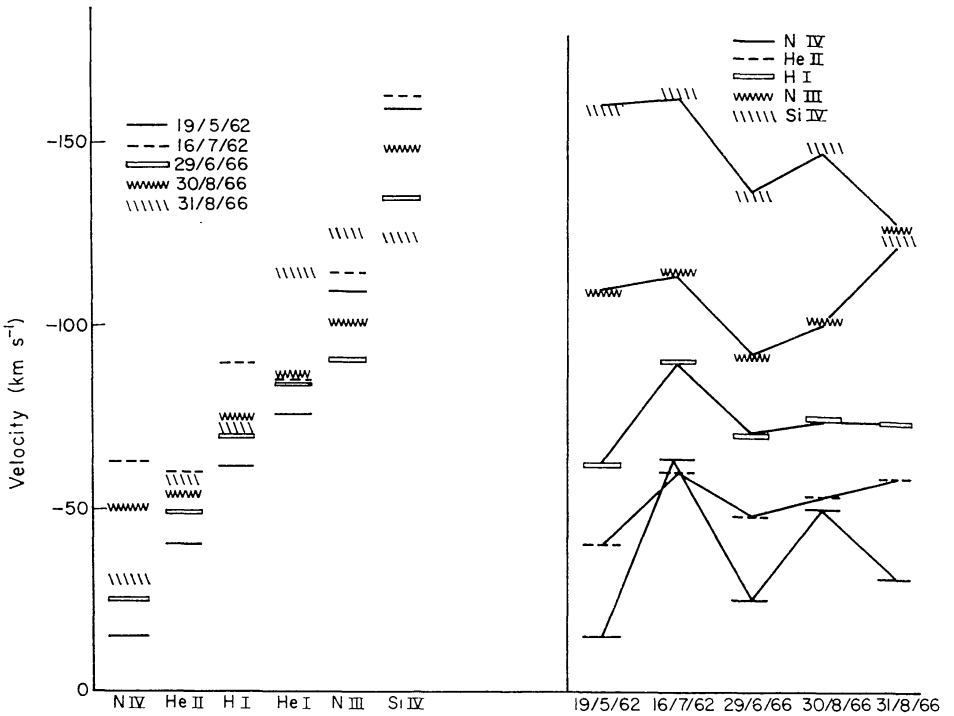

FIG. 9. *Mean absorption velocities of ions in HD* 152408.

He I. As in the case of HD 152236 these lines present the most interesting information about the outer atmosphere. All the strongest lines from the 2 ^3P level are found in emission, indicating that they are formed at dilutions of 0·1 and lower. The emission velocities of the three main lines, 4471, 4026 and 3819 are fairly close (lying from 60 to 80 km s^{-1}) and the absorption velocities are generally higher than the mean He I value (see table above). The velocities decrease in order 4471, 4026, 3819 as may be expected from lines of decreasing strength in an atmosphere accelerating outwards. The line at 4120 is present, probably with

weak emission, but measurements were prevented by the strength of Si IV 4116 in emission. The line at 3705 is also present, stronger than other He I lines in the region, but badly blended with the Balmer line H 16. There are indications of an emission component. 4713 is weak with very variable emission.

Of the 2 ^1P lines 4387 is present weakly with variable emission. Velocities are unreliable but appear to be close to the He I mean. This is not surprising as these lines start to form emission components at dilution values of about 0·5. The line 4921 is seen to be almost totally in emission in some lower dispersion plates. The strongest 2 ^1S line, 3964, has also a weak emission component. This should be formed at W 0·1 to 0·2, which is consistent with the absorption velocities being greater than the He I mean.

The most important lines are the 2 ^3S lines, 3888 and 3187, which are expected to tell us about the outermost regions of the atmosphere. However, instead of the 3888 line there is the strong unidentified line at 3880 (see table) and an emission ' band ' from 3890 to about 3900. The feature in all five plates is shown in Fig. 10.

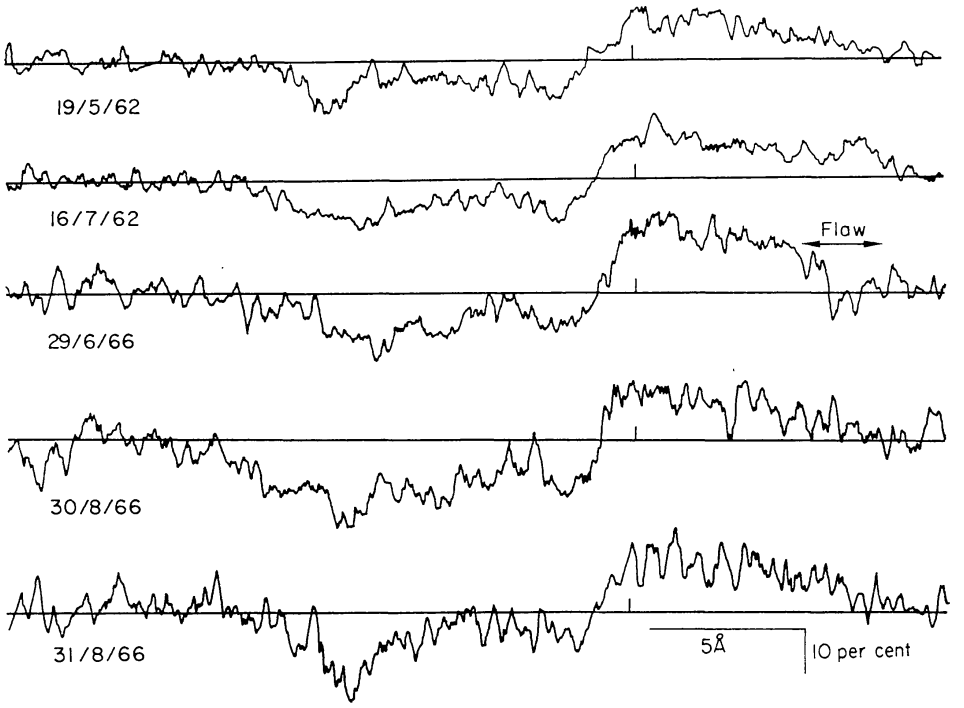

FIG. 10. *Absorption and emission feature* 3880–3890 *Å in HD* 152408.

These profiles may be compared with those of WR stars (e.g. Underhill 1959). In all cases the strongest absorption feature is the highly blue-shifted 3888 line which is expected to form an emission component only at extremely low values of dilution. It is chiefly from this line that the expansion velocities of WR stars are deduced to be of the order of 1000 km s^{-1}. In WR stars, the line is in fact accompanied by a broad emission band, as shown in some examples in Fig. 11. Mention should also be made of the very peculiar Be star BD +11° 4673, studied by Merrill (1951). The spectrum has very wide emission features and has no real spectral classification. However, the line 3888 displays very variable and high velocity shifts to the blue, sometimes forming six components with velocities up to 400 km s^{-1}. The He I lines 3447, 3613, 3819, 3965, 4026 and 4471 are also reported

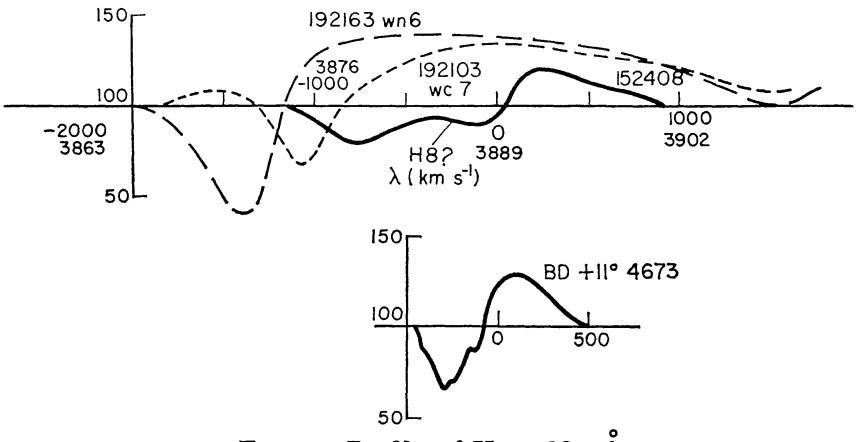

FIG. 11. *Profiles of He* I 3889 *Å.*

to have similar but less strong behaviour occasionally. Fig. 11 shows a typical 3888 profile from this star.

The strongest 2 ^3P lines in WR stars sometimes have absorption components similarly blue-shifted. On inspection, the strong 2 ^3P lines in HD 152408 were found to have fairly strong asymmetrical absorption extending several angstroms shortward of 4471, 4026, and possibly 3819. Some of these are shown in Fig. 12. The spectrograms do not permit measurement of the 3187 line.

It is therefore proposed that the unidentified strong line at 3880 is the He I 3888 line formed high in the atmosphere in a region which is expanding at some 600 km s^{-1}. The absorption is in fact smeared in velocity from near zero up to 800 km s^{-1}, indicating an increase in velocity with height, although the sharp dip near 600 km s^{-1} must mean that a plateau is formed somewhere. The velocity

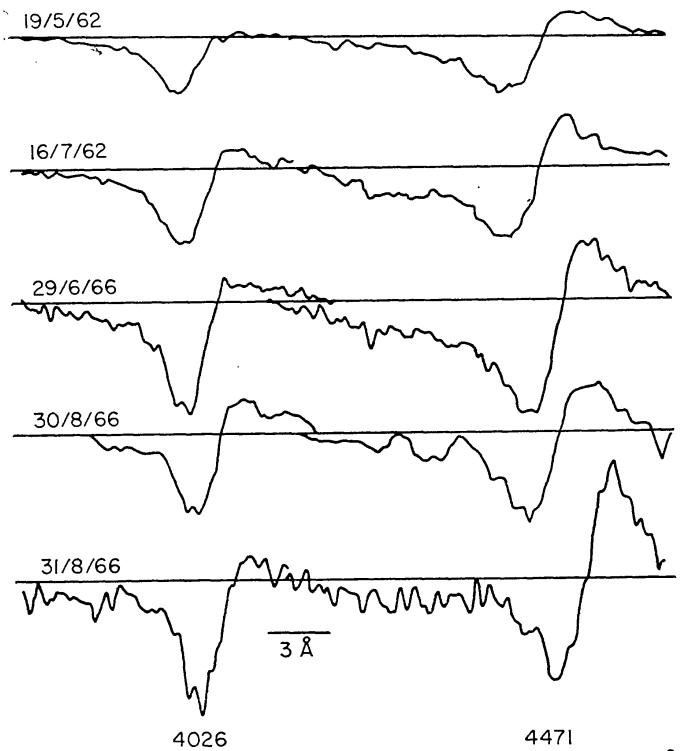

FIG. 12. *HD* 152408. *Unreduced profiles of He* I *lines* 4026 *and* 4471 *Å, showing strong shortward absorption.*

plateau appears to shift from plate to plate. The lines 4471 and 4026 also have components suggesting expansion velocities of several hundred km s^{-1}, with a possible dip at about 600 km s^{-1}.*

Finally, inspection of the Balmer lines showed that on the 31/8/66 plate many of them have a series of shortward absorption components, again indicating expansion velocities of several hundred km s^{-1}. The table below gives all the high velocity data for this star. Columns *a* and *b* indicate the velocities of the absorption centre and the maximum extent of the absorption, respectively. Figures in brackets have half weight.

	3888·6		4471·6		4026·3		3819·6	
	a	*b*	*a*	*b*	*a*	*b*	*a*	*b*
19/5/62	−725	(−840)	−435	(−740)	—	−520	—	(−440)
16/7/62	−655	−750	−475	−725	—	−620	—	(−500)
29/6/66	−595	−925	−570	−910	−335	−665	—	(−390)
30/8/66	−670	(−1100)	(−450)	−885	(−340)	−475	—	−600
31/8/66	−665	(−655)	(−210)	−905	−290	−865	—	−460
			−595		−495			

Balmer lines in 31/8/66 plate:

Hβ—broad dips at −1350 km s^{-1} and (smaller) −660 km s^{-1}.

Hγ—absorption at −630 km s^{-1}, not present on other plates.

The blue-shifted absorption of the 3819 line is blended with He I 3813. The feature is considered to be caused by blue-shifted absorption because the measured velocity is not typical of He II and the strength of the feature is greater than that expected for the He II lines.

The spectrum of the Of star HD 151804 which has a much weaker shell spectrum is useful for comparison with HD 152408. The spectrum of HD 151804 shows He I 3888 in its expected position, and no marked asymmetry in the other He I and Balmer lines.

The question now arises of whether the observed features and changes mean that the star is a binary. The WR type undulations in the continuum, the strong emission lines and highly shifted absorptions are all variable. The crux of the argument is the 3880 line. If there is a faint WR companion this line must belong to it, together with the shortward absorptions of 4471 etc. The presence of these absorptions mean that light is absorbed from the spectrum of the primary, an improbable situation as the secondary cannot always mask the primary and have about the same velocity relative to it. In any case the normally positioned 3888 line should be present in all cases. We are left with the possibility that the primary and secondary stars are of comparable magnitude, which makes it strange that the star has not been identified as a variable. In addition, the secondary spectrum would be odd, containing weak emission bands, emission lines of N III, Si IV, H I and He I, and with highly displaced He I lines.

A far more reasonable assumption is that the star is single, with an outward flowing and rapidly expanding outer atmosphere in which conditions approach those found in WR atmospheres. The state of the outer atmosphere is presumably very unstable and variable and at velocities of 500 km s^{-1} the outer atmosphere could regenerate itself completely in a matter of hours.

* The possibility of these features being blends of other lines is discounted on account of (1) the similarity of the shortward absorption in all the lines, and (2) the absence of any probable lines in the regions concerned.

The Balmer lines. These form a progression in velocity as in HD 152236. However, the broadness of the lines and probably greater mass motion in the atmosphere itself makes the series less clear in this star. Hβ is entirely in emission, apart from an absorption feature at 280 km s^{-1} on 31/8/66 and those noted above, Hγ has a strong emission component in all cases, with a secondary emission peak at about 4345 Å. It is possible that this is caused by O II emission, but unlikely in such strength as it is not strongly represented anywhere else in the spectrum. Hδ is seriously blended with N III 4103 in all cases and its velocities are not to be trusted. Hϵ is the last Balmer line with clear redward emission (not always measured because of its faintness). The dilutions of the line forming regions are put at: Hϵ $W = 0{\cdot}3$ to Hβ at $0{\cdot}1$ or less.

The lines of Si IV *and N* III. Their high velocities and the strength of the emission components suggest that these lines are not formed in the lower layers of the atmosphere as one might normally expect. If they are formed at the same height as the stronger Balmer and He I lines there must be extreme deviations from conditions of thermodynamic equilibrium. In the case of Si IV it appears that the enhanced emissions are caused by populating the upper levels by strong UV absorption, with subsequent cascade through the levels, producing the lines 4328 and 4314; 3762 and 3773; 3165 and 3149; and 4088 and 4116. The outstanding emission lines in the N III spectrum are the group at 4640 and those near Hδ, which form two steps of a cascade. In addition to the cascade cycle, Bowen has proposed a fluorescence mechanism (Hynek 1951) for the formation of these lines. The upper level of the 4640 lines can be populated by an almost resonant absorption of O III emission at 374 Å, a coincidence which may well be the chief cause of the extraordinary strength of these lines. For these cycles to work effectively a dilution value of about $0{\cdot}1$ is required so that the lines are formed in a high part of the atmosphere. These high excitation states must arise from metastability, or preferential photoionization processes occurring in a dilute radiation field. We note here that in the Orion B stars Morton (1967) has observed the Si IV resonance lines in his rocket UV spectra with velocity shifts of some thousands of km s^{-1} and these presumably also arise at great heights in the stellar atmospheres.

There are no Si V ions present, as may be expected, the ionization potential being 165 V. N IV is found in absorption, contrary to the finding of Swings (1942). Measured velocities are low and irregular, suggesting that the ion is situated mainly in the lower atmospheric layers.

Other lines. The He II lines 4686 and 3203 from the 3 ^2D level are both strongly in emission, presumably as a result of absorption in two strong UV lines. Resonant absorption of Lyman α (1215 Å) which must be strong in the outer atmosphere certainly contributes a large portion of the great strength of the 4686 line. The observed absorption component of 3203 has a high velocity and a considerable shortward wing extending to 400 to 500 km s^{-1}. It appears therefore that the lines are formed at great height in the atmosphere. The remainder of the lines (Pickering series) are entirely in absorption and their consistently low velocities show that they are formed low in the atmosphere, as expected from their high excitation potentials. There is no measurable progression in velocity in the stronger members of the series and is assumed that the velocity does not alter significantly over the range of their formation. The series is visible down to $n = 22$ (3760 Å) but is weak enough not to interfere with the Balmer line measurements.

C III and O III are weak in all spectrograms. The weakness of C III indicates that the star is related to the W–N class of stars rather than the W–C. C III is however seen in emission at 4650, which is where the strongest emission band is found in W–C stars. The only other instance of this emission in an Of star was reported recently by Thackeray & Walker (private communication) in HD 153919. O III is measured in absorption only but is almost certainly present in the blended emission lines in the region 3300–3400 Å. The strongest line is slightly obscured by the Si IV emission at 3762 Å. The velocities appear to be intermediate between those of He II and He I absorption lines, placing it in the expected height range.

A number of weak lines, quite unsuitable for radial velocity measurement, are identifiable as Fe III, Ne II and O III. The strongest lines of N III, Si IV and He II all show significant variation in emission strength, although the line widths do not change very much.

Interstellar lines. There are several faint interstellar lines in the spectrum, and not all were measured for velocity. Dunham's Ti II (3383) was measured at -19, -18, and -8 km s^{-1}, while the mean of the Ca H and K velocities is -10 km s^{-1} with a standard deviation of 4. The H and K lines show structure but the velocities of the satellites are all below 40 km s^{-1} suggesting that they are probably not stellar.

The atmosphere of HD 152408. From the above discussion it is evident that the atmosphere of HD 152408 is being accelerated away from the star in a similar way to that of HD 152236, but more violently. It is more difficult to construct velocity–height and temperature–height relationships, especially as it is evident that these can change to a certain extent in a short time.

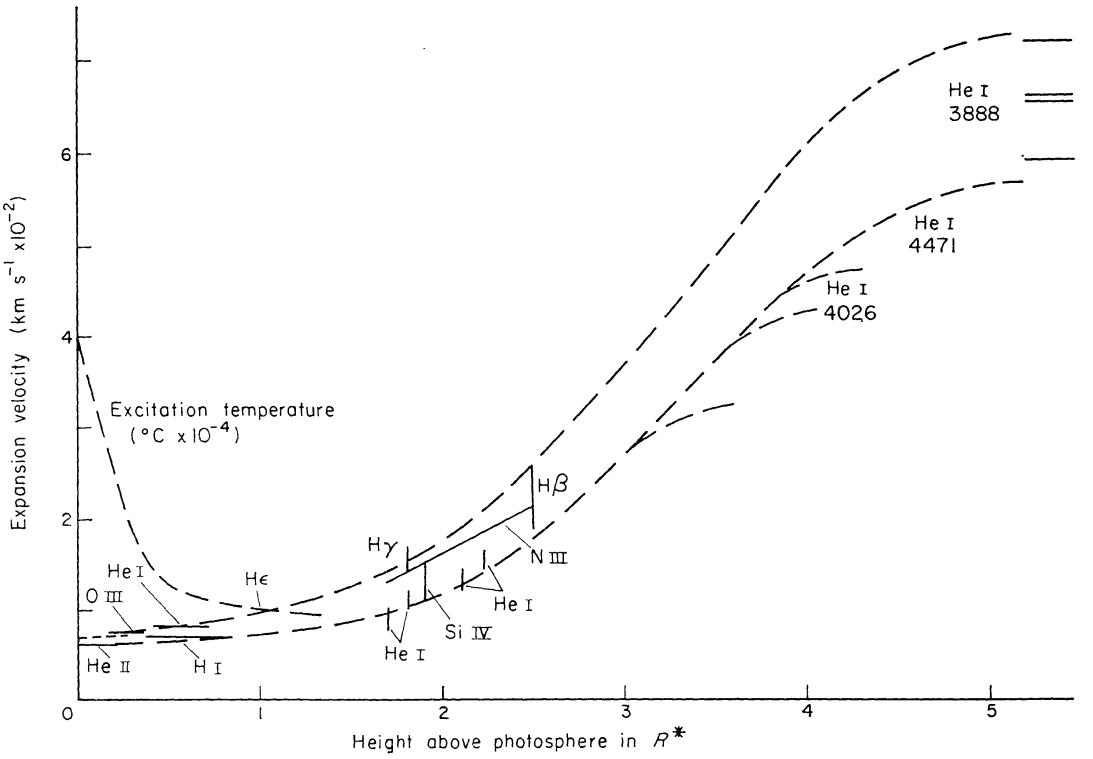

FIG. 13. *Deduced velocity field of HD* 152408.

The radial velocity of the star itself is probably not very different from that of the cluster NGC 6231 (about -30) and the star is not a high-velocity runaway star as supposed (e.g. by Blaauw 1961) from the high velocity of its strong lines. It is assumed therefore that the atmosphere near the stellar surface (closer than $1{\cdot}1\ R_*$) moves away from the star relatively slowly (<30 km s^{-1}). As in the case of HD 152236 the strong He I lines and Balmer lines and also the Si IV and N III lines, indicate that further out there is a region of strong acceleration and then a plateau of velocity in the region of 600 km s^{-1}. As He I 3880 has an associated emission band the radiation in this outer region must be very dilute and its source may be several stellar radii away from the star. Fig. 13 shows the proposed mean atmospheric structure deduced from the five plates.

HD 151804. Spectrum O7f to O9f, half a degree from the nucleus of NGC 6231 and somewhat closer to HD 152408; $m_v = 5{\cdot}2$ and M_v about -7. Four high dispersion spectrograms and four prismatic spectrograms (29 Å/mm at Hγ, unmeasured) were available. This star is mentioned in the same discussion as HD 152408 (Swings 1942; Struve 1944) and noted for its similarity to that star. The shell lines are not so pronounced as in HD 152408 although there is variation in the emission strength of the lines near Hδ. There is no highly displaced 3888 line. The picture obtained is similar to that of HD 152408, with a less extensive and more slowly moving atmosphere, but liable to outbursts of activity which excite the shell emission spectrum. The continuum of the spectrum also shows enhanced regions, similar to W–N emission bands, and varying in intensity.

Struve remarked that the O III 3759 line in this star has a typical P Cygni structure. It appears to be much more likely that the emission observed is that from Si IV 3762, as measured here and in HD 152408. Swings reported emission at Hα, He I 5875 and C III 5696, in the longer wavelengths not covered here.

The measured line velocities, corrected for the Earth's motion are given in the table below. Accuracy of measurements is ± 8 km s^{-1} per line as for HD 152408. Rubin (1962) gives the velocity of this star as $-62{\cdot}5$ km s^{-1}.

The mean velocities of pure absorption lines of various elements and ions, with the numbers of lines measured in brackets, are as follows:

	21/3/62	17/4/62	2/7/66	31/8/66
H I	-49 ± 3 (7)	-44 ± 2 (7)	-52 ± 4 (8)	-51 ± 5 (7)
He I	-41 ± 5 (5)	-36 ± 4 (6)	-47 ± 4 (9)	-53 ± 5 (5)
N III	-46 ± 6 (5)	-36 ± 3 (7)	-45 ± 2 (7)	-52 ± 3 (8)
N IV	-38 ± 15 (2)	-25 ± 7 (3)	-48 ± 4 (3)	-19 ± 9 (2)
He II	-22 ± 5 (3)	-33 ± 15 (3)	-36 ± 11 (3)	-42 ± 7 (6)
O III	-40 ± 8 (4)	-33 ± 5 (4)	-50 ± 6 (4)	-48 ± 12 (3)

The H I lines here are the most reliable lines beyond Hϵ and the tabulated He I velocities omit 4471 and 3888 (and 4026 where discrepant). These figures again differ significantly between plates and between ions. The values of Si IV are high and they too show the greatest tendency to emission.

The emission lines. There are far fewer emission lines in the spectrum of this star than in HD 152408. Lines appearing in emission are: Hβ, Hγ (marginally) N III 4634–41, 4097, 3938 (3942 occasionally); Si IV 4116, 4088, 3773, 3762, 3149, 3165; He II 4686; C III 4647–50, and the unidentified lines at 4485 and 4503. He I is not found in emission in the blue. This suggests an atmosphere extending

TABLE III

HD 151804. *Measured velocities of spectral lines*

Identification		λ	Velocities of lines or measured λ 21/3/62	17/4/62	2/7/66	31/8/66	Remarks
Ti II		3383·76	−16	+3	−20	—	Sharp, interstellar
N IV		3478·69	−24	−12	−45	—	—
N IV		3482·98	(−67)	−36	−54	−11	—
N IV		3484·90	—	(−28)	−45	−28	Weak, blended
He I		3587·3	−38	(−13)	−53	—	—
		—	—	—	3581·0	—	Identity?
He I		3634·3	−47	−45	−61	—	—
H 17		3697·15	(−20)	3693·6†	—	—	† Identity?
		—	3703·4	3703·4	3704·0	3704·0	Strong blend of H 16, He I, O III
H 15		3711·97	(−28)	(−20)	−27	(−20)	—
H 14		3721·94	−52	−44	−51	−60	—
H 13		3734·37	−60	−35	−58	−68	—
H 12		3750·15	−44	−43	−55	−44	—
O III		3754·67	−28	−19	−67	—	—
O III		3757·21	−28	−35	−43	−36	—
O III		3759·87	−60	−43	−51	−60	—
Si IV	e	3762·4	−28	−19	−43	—	—
H 11		3770·63	−43	−43	−51	−44	—
Si IV	e	3773·13	+4	+5	−19	—	—
O III		3791·26	−44	−34	−41	−25	—
H 10		3797·90	−51	−42	−50	−36	—
He II		3813·5	—	—	(−3)	−60	Weak
He I		3819·61	−36	−34	−58	−28	—
He II		3833·83	—	—	—	(−12)	Blended with H 9

1968MNRAS.141..219H

TABLE III (*continued*)

Identification		λ	Velocities of lines or measured λ 21/3/62	17/4/62	2/7/66	31/8/66	Remarks
H 9		3835·39	−58	−42	−65	−51	—
He II		3858·07	−19	−63	(−19)	−52	—
He I		3867·6	—	3864·3†	−42	—	† Blend?
He I		3888·65	−57	—	−42	(−125)	Bad blend with H 8
H 8		3889·05	(−34)	−56	−55	(−62)	Bad blend with He I
He II		3923·5	−26	−10	−57	−20	—
		—	—	3902·1	—	—	Identity?
Ca II		3933·67	−2	−9	−11	−5	Interstellar
N III	e	3934·41	+5	—	−28	—	—
N III	e	3938·52	+5	−25	+6	—	—
N III	e	3942·75	(+104)	—	—	—	Very weak
		—	3961·1	3961·1	3961·0	—	Identity?
He I		3964·73	−25	−25	−49	—	—
Ca II		3968·48	+5	−1	−3	−5	Interstellar
Hε		3970·13	−55	−85	−42	−66	—
He I		4026·3	−62	−60	−55	−58	—
Si IV		4088·86	−81	−59	−70	−79	Emission present
N III		4097·31	−116	−88	−91	−64	Emission present
Hδ		4101·75	−45	−30	−84	−35	Emission present, blended with N III 4103·37
Si IV		4116·11	−89	−59	−91	−118	—
	e	—	+65	—	—	+45	—
He I		4120·9	(−150)	−23	−40	−57	Shallow line
He I		4143·76	—	−44	—	—	—
N III		4195·70	(−130)	(−15)	—	—	Shallow line
He II		4199·87	—	—	—	(−50)	Blended with N III
N III		4200·02	(−50)	−36	−54	−55	Blended with He II
	e	—	—	—	4221·7	—	Identity?

TABLE III (*continued*)

Identification		λ	Velocities of lines or measured λ 21/3/62	17/4/62	2/7/66	31/8/66	Remarks
Hγ		4340·47	−115	−76	−106	−103	—
	e	—	—	—	—	+145, +75	Emission weak
N III		4379·09	−60	−33	−51	−48	—
He I		4387·93	−39	−47	−45	−62	—
		—	—	—	4416·3	—	Identity?
Band		4430	4428·4	4427·7	4427·2	4433·0	Interstellar
He I		4471·6	−72	−53	−64	−68†	† Shortward wing to −330
Mg II		4481·23	−53	—	(−25)	—	Identity?
	e	4485·7	−25	−32	−30	−15	Unidentified. From Underhill (1966)
	e	4503·7	+8	−32	+8	−48, +25	Unidentified. From Underhill (1966)
N III		4510·92	−38	−39	−45	−48	—
N III		4514·89	−44	−39	−44	−48	—
N III		4518·18	—	−52	−44	−48	—
N III		4523·60	−31	−26	−38	−41	—
N III		4534·56	−59	−26	−38	−68	—
He II		4541·61	−25	−25	−31	−48	—
N III	e	4634·16	−5	—	−17	−28	Very strong
N III	e	4640–41	(−30)	—	(−37)	(−28)	Very strong
C III		4647·40	—	—	—	−86	—
	e	—	+2	—	—	—	—
C III		4650·16	—	—	—	−67	—
	e	—	(+60)†	—	—	—	† End of plate
He II		4685·75	—	—	—	−320†	† Diffuse absorption centre
	e	—	—	—	−24	+4	Very strong
He I		4713·15	—	—	−24	−60	—
Hβ		4861·33	—	—	−141	—	—
	e	—	—	—	+107	+34	—

to 1 or 2 radii above the photosphere, as that of HD 152236, but with considerably higher excitation temperature. Observations in the red (He I 5875, 6678, and Hα) would undoubtedly be of great use in determining the outer atmospheric velocities but they are not at present available. The strong emissions at 4634, 4640, 4686 have shortward dips which may be absorption features. This is particularly distinct in the line 4686 on 31/8/66.

The He I spectrum on these plates yields little information. 3888 is badly blended with H9 in all cases and often appears to have two or more absorption centres. From its low velocities we conclude that the line is formed low in the atmosphere. Presumably the density of the atmosphere at low values of W is insufficient to form the line in any strength. The shortward absorption of 4471 has variable strength, and indicates velocities extending to some 300 km s^{-1}.

The Balmer lines do not form a clear progression in velocity and it appears that the atmospheric expansion velocity is low below the level of Hγ. Hδ is as usual blended with N III 4103. From its emission strength Hβ is placed at W approximately 0·3.

Of the strong lines of Si IV and N III, the former have the greater tendency to emission, as found in HD 152408, although velocities suggest that they may be formed slightly lower in the atmosphere. The lines certainly have variable weak emission components and must be formed at dilution values of about 0·3, where the cascade mechanism begins to be effective. Assuming tentatively that the velocities of 300 km s^{-1} are real for great heights in the atmosphere, the velocity field in Fig. 14 is proposed, which resembles a scaled-down version of HD 152408.

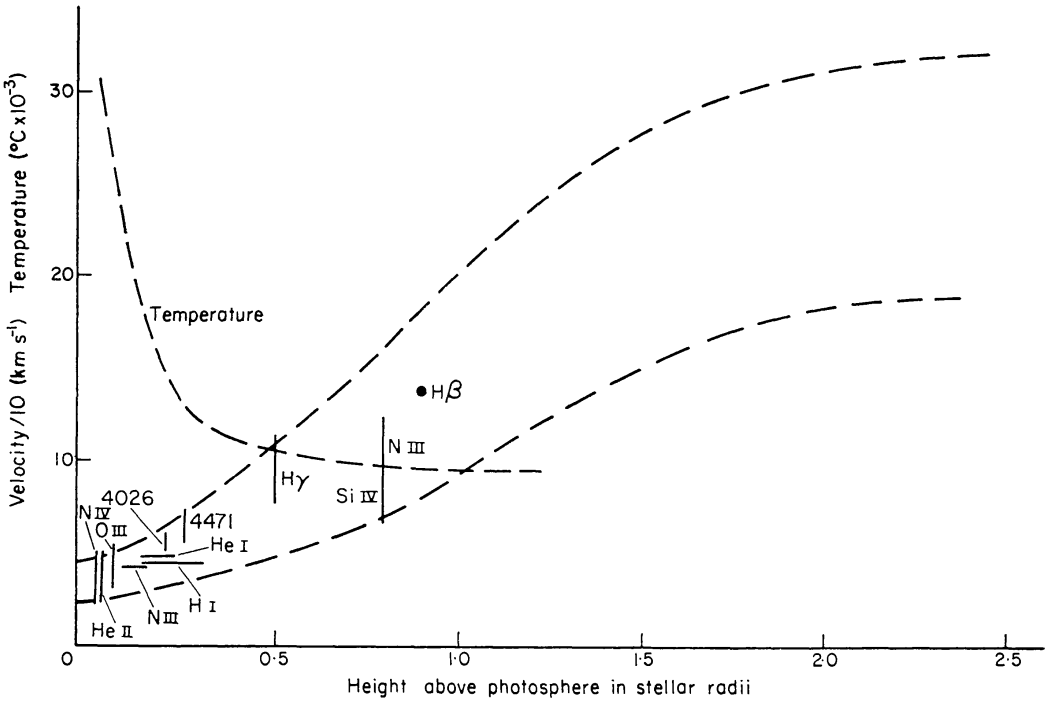

FIG. 14. *HD* 151804. *Deduced temperature and velocity fields.*

The high velocity values are very tentative, but it seems probable that there is velocity streaming in this star too.

The strong Ca II *lines.* These do not add much to the picture of the expanding atmosphere, being again almost entirely interstellar, but are fairly distinctive in

having a strong satellite at about -40 km s^{-1} with respect to the line centre. This velocity is too low to fit into the proposed atmospheric field and it must again be regarded as being that of an interstellar gas cloud.

Conclusion. The study of these three high luminosity early-type stars has indicated that each one has an extended expanding atmosphere. The O stars have more extended atmospheres, expanding at greater velocities, but it is not possible to decide whether this may be primarily caused by surface gravity, temperature, rotation or luminosity. Fragmentary evidence suggests that such moving outer envelopes may be common in high luminosity early type stars. The strongest other evidence is that of Morton (1967) whose UV rocket spectra of Orion B supergiants, which are standard stars of their type, show resonance absorption lines displaced by several thousand km s^{-1}. More recent UV spectra by Morton (private communication) show strong lines arising from excited levels which have velocities about half those of the resonance lines. This suggests that the acceleration deduced here may continue to much higher velocities. It is proposed to discuss the implications of this further, and to derive more exact atmospheric models in a later paper.

Acknowledgments. I wish to thank Dr A. D. Thackeray for the loan of many of the plates used and for making facilities available for obtaining others in 1966. I am grateful to Dr D. W. Peat for making the 1966 observations. This work was partly supported by a CSIR grant awarded through the University of the Witwatersrand.

The Observatories,
Madingley Road,
Cambridge.
1968 *February.*

References

Blaauw, A., 1961. *Bull. astr. Insts Neth.*, **15,** 265.
Buscombe, W., 1962. *Mon. Not. R. astr. Soc.*, **124,** 189.
Code, A. D. & Houck, T. E., 1958. *Publs astr. Soc. Pacif.*, **70,** 261.
Cousins, A. J., 1952. *Observatory*, **72,** 86.
Eggen, O. J., 1958. *R. Obs. Bull.*, No. 41E.
Evans, D. S., Menzies, A. & Stoy, R. H., 1959. *Mon. Not. R. astr. Soc.*, **119,** 638.
Gaposchkin, S. & Payne, C., 1938. *Variable Stars*, p. 329, Harvard Observatory.
Hutchings, J. B., 1966. *Mon. Not. R. astr. Soc.*, **132,** 433.
Hynek, J. A. (ed.), 1951. *Astrophysics*, p. 104, McGraw Hill, London.
Menzel, D. H., 1937. *Astrophys. J.*, **85,** 330.
Menzel, D. H. & Baker, J. G., 1937. *Astrophys. J.*, **86,** 70; 1938. *Astrophys. J.*, **88,** 422.
Merrill, P. M., 1949. *Astrophys. J.*, **110,** 420; 1951. *Astrophys. J.*, **114,** 338.
Morton, D. C., 1967. *Astrophys. J.*, **147,** 1017.
Rosseland, S., 1926. *Astrophys. J.*, **63,** 218.
Rubin, A. J. *et al.*, 1962. *Astrophys. J.*, **67,** 491.
Sanford, R. F., 1947. *Astrophys. J.*, **105,** 222.
Struve, O., 1944. *Astrophys. J.*, **100,** 189.
Swings, P., 1942. *Astrophys. J.*, **95,** 112.
Underhill, A. B., 1959. *Publs Dom. astrophys. Obs.*, **11,** 209.
Underhill, A. B., 1966. *The Early Type Stars*, Reidel Co.
Wellman, P., 1951. *Z. Astrophys.*, **30,** 71, 88; 1955. *Vistas Astr.*, **1,** 303.
Wilson, R. E., 1953. *General Catalogue of Stellar Radial Velocities*, Carnegie Publ. 601.